EPJ Web of Conferences **73**, 02013 (2014)
DOI: 10.1051/epjconf/20147302013

Phase-space distributions and orbital angular momentum

B. Pasquini[1,2,a] and C. Lorcé[3,4,b]

[1]Dipartimento di Fisica, Università degli Studi di Pavia, Italy
[2]INFN, Sezione di Pavia, 27100 Pavia, Italy
[3]IPNO, Université Paris-Sud, CNRS/IN2P3, 91406 Orsay, France
[4]IFPA, AGO Department, Université de Liège, Sart-Tilman, 4000 Liège, Belgium

Abstract. We review the concept of Wigner distributions to describe the phase-space distributions of quarks in the nucleon, emphasizing the information encoded in these functions about the quark orbital angular momentum.

1. Introduction

The concept of Wigner functions met a renewed interest in the context of QCD to describe the phase-space distributions of partons in the nucleon [1–4]. These functions represent the quantum mechanical analogues of the classical phase-space density, but do not share with them a probabilistic interpretation. This intrinsic limitation is due to the Heisenberg uncertainty principle which prevents knowing simultaneously the position and momentum of a quantum-mechanical system. Despite that, the physics of Wigner distributions is very rich and one can try to select certain situations where a semiclassical interpretation is still possible. In Sect. 2, after introducing the formal definition of the quark Wigner distributions, we will discuss, as an example, the physical picture that emerges within a light-front constituent quark model (LFCQM) for the Wigner distributions of unpolarized quarks in a unpolarized nucleon. In Sect. 3, we will present the model-independent relation between the quark orbital angular momentum (OAM) and the Wigner distribution for unpolarized quarks in a longitudinally polarized nucleon.

2. Quark Wigner distributions

The quark Wigner distributions are defined in terms of the matrix elements of the Wigner operators $W^{[\Gamma]q}$ sandwiched between nucleon states with polarization $\vec{S}$ as follows

$$\rho^{[\Gamma]q}(\vec{b}_\perp, \vec{k}_\perp, x, \vec{S}) \equiv \int \frac{\mathrm{d}^2\vec{\Delta}_\perp}{(2\pi)^2} \langle p^+, \tfrac{\vec{\Delta}_\perp}{2}, \vec{S}|\widehat{W}^{[\Gamma]q}(\vec{b}_\perp, \vec{k}_\perp, x)|p^+, -\tfrac{\vec{\Delta}_\perp}{2}, \vec{S}\rangle, \tag{1}$$

[a]e-mail: pasquini@pv.infn.it
[b]e-mail: lorce@ipno.in2p3.fr

with

$$\widehat{W}^{[\Gamma]q}(\vec{b}_\perp,\vec{k}_\perp,x) \equiv \frac{1}{2}\int \frac{\mathrm{d}z^-\,\mathrm{d}^2\vec{z}_\perp}{(2\pi)^3}\, e^{i(xp^+z^- - \vec{k}_\perp\cdot\vec{z}_\perp)}\,\overline{\psi}^q(y-\tfrac{z}{2})\Gamma\mathcal{W}\,\psi^q(y+\tfrac{z}{2})\big|_{z^+=0}. \tag{2}$$

Here and in the following, for a generic four-vector $a=[a^+,a^-,\vec{a}_\perp]$ we use the light-front components $a^\pm = a\cdot n_\mp$, with the two lightlike four-vector $n_\pm$ satisfying $n_+\cdot n_- = 1$, and the transverse components $\vec{a}_\perp = (a^1,a^2)$. Furthermore, in Eq. (2) ψ^q is the quark field operator, p^+ is the nucleon longitudinal momentum, $x = k^+/p^+$ is the fraction of nucleon longitudinal momentum carried by the active quark, and $y^\mu = [0,0,\vec{b}_\perp]$. The superscript Γ stands for any twist-two Dirac operator $\Gamma = \gamma^+, \gamma^+\gamma_5, i\sigma^{j+}\gamma_5$ with $j=1,2$. A Wilson line $\mathcal{W}\equiv\mathcal{W}(y-\frac{z}{2},y+\frac{z}{2}|n_+)$ ensures the color-gauge invariance of the Wigner operator, connecting the points $(y-\frac{z}{2})$ and $(y+\frac{z}{2})$. Using a transverse translation in Eq. (1), we find

$$\rho^{[\Gamma]q}(\vec{b}_\perp,\vec{k}_\perp,x,\vec{S}) = \int \frac{\mathrm{d}^2\vec{\Delta}_\perp}{(2\pi)^2}\, e^{-i\vec{\Delta}_\perp\cdot\vec{b}_\perp}\, W^{[\Gamma]q}(\vec{\Delta}_\perp,\vec{k}_\perp,x,\vec{S}), \tag{3}$$

where $W^{[\Gamma]q}$ are the quark-quark correlators defining the generalized transverse-momentum dependent parton distributions (GTMDs) [5–8] for $\Delta^+=0$

$$\begin{aligned} W^{[\Gamma]q}(\vec{\Delta}_\perp,\vec{k}_\perp,x,\vec{S}) &= \langle p^+,\tfrac{\vec{\Delta}_\perp}{2},\vec{S}|\widehat{W}^{[\Gamma]q}(\vec{0}_\perp,\vec{k}_\perp,x)|p^+,-\tfrac{\vec{\Delta}_\perp}{2},\vec{S}\rangle \\ &= \frac{1}{2}\int \frac{\mathrm{d}z^-\,\mathrm{d}^2\vec{z}_\perp}{(2\pi)^3}\, e^{i(xp^+z^- - \vec{k}_\perp\cdot\vec{z}_\perp)}\,\langle p^+,\tfrac{\vec{\Delta}_\perp}{2},\vec{S}|\overline{\psi}^q(-\tfrac{z}{2})\Gamma\mathcal{W}\,\psi^q(\tfrac{z}{2})|p^+,-\tfrac{\vec{\Delta}_\perp}{2},\vec{S}\rangle\big|_{z^+=0}. \end{aligned} \tag{4}$$

This means that the Wigner distributions are the two-dimensional Fourier transforms of GTMDs. Contrary to all the other distribution functions, the GTMDs are in general complex-valued functions. However, thanks to the hermiticity property of the GTMDs correlator, the two-dimensional Fourier transforms of the GTMDs are always real-valued functions, in accordance with their interpretation as phase-space distributions. Counting the possible values for the nucleon polarization $\vec{S}$ and the quark polarization states, one finds 16 independent Wigner distributions at leading twist. Here, as an example, we discuss the results in a LFCQM [3, 8] for the most simple case with unpolarized quarks in an unpolarized nucleon. Furthermore, we consider the first moments in x of the Wigner functions, corresponding to transverse distributions in the $(\vec{b}_\perp,\vec{k}_\perp)$ space. In Fig. 1, we show the results for the distribution of u quarks in the transverse-position space, for fixed value of $k_\perp = |\vec{k}_\perp| = 0.3$ GeV. The distribution in the left upper (lower) panel is obtained with the direction of the quark transverse momentum parallel (antiparallel) to the transverse position vector, while the quark transverse motion has only polar components, pointing anti-clockwise (clockwise) in the right upper (lower) panel. We observe that the size of the distributions is the same when the flux of momentum is inwards or outwards, otherwise the quarks would not form a stable bound system. Analogously, the distributions are equal when the orbital motion of the quarks is clockwise or anti-clockwise, indicating there is no net OAM for unpolarized quarks in an unpolarized nucleon. On the other hand, the distributions have different widths in the case of radial and orbital motion of the quarks. In particular, the configuration with $\vec{k}_\perp \perp \vec{b}_\perp$ is favored with respect to the configuration with $\vec{k}_\perp \parallel \vec{b}_\perp$. This can be understood with naive semiclassical arguments. The radial momentum of a quark is expected to decrease rapidly in the periphery because of confinement. The polar momentum receives a contribution from the orbital motion of the quark which can still be significant in the periphery, since in an orbital motion, one does not need to reduce the momentum to avoid a quark escape. Similar behavior is observed for the distributions of d quarks [7], with the difference that the spread of the distributions is smaller for u quarks than for d quarks. This reflects the fact that u quarks are more concentrated at the center of the proton, while the d-quark distribution has a tail which extends further at the periphery of the proton.

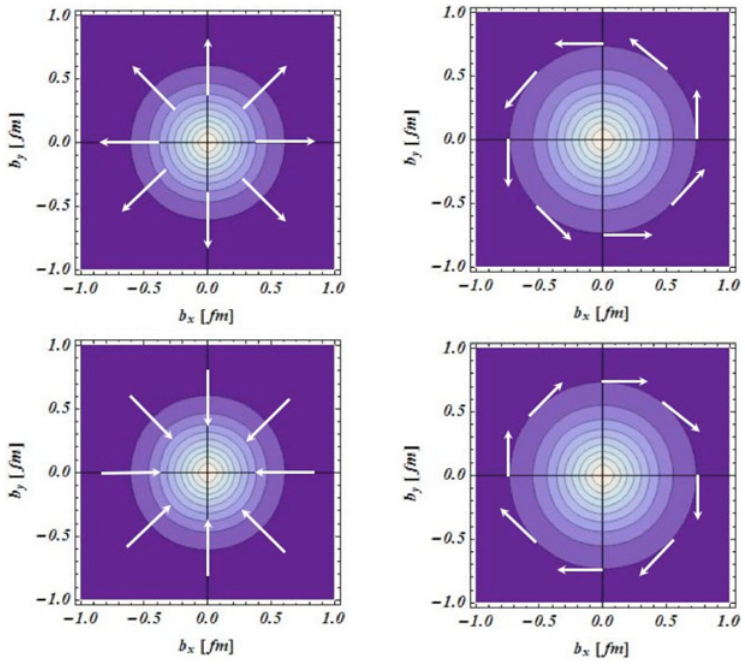

Figure 1. The Wigner distribution for unpolarized u quarks in an unpolarized nucleon in impact parameter space, with different orientations for $\vec{k}_\perp$ at fixed value of $k_\perp = 0.3$ GeV. Left panels: the transverse momentum has only radial components, parallel (upper panel) and antiparallel (lower panel) to the position vector in the transverse plane $\vec{b}_\perp$. Right panels: the transverse momentum has only polar components, pointing anti-clockwise (upper panel) and clockwise (lower panel). The arrows represent the vector $\vec{k}_\perp$ at a given value of $\vec{b}_\perp$.

3. Quark orbital angular momentum

The Wigner distributions allow us to obtain a very intuitive representation for the quark OAM [3, 4]:

$$\ell_z^q = \int \mathrm{d}^2\vec{b}_\perp \left(\vec{b}_\perp \times \langle \vec{k}_\perp \rangle^q\right)_z , \tag{5}$$

where $\langle \vec{k}_\perp \rangle^q$ is the distribution in impact-parameter space of the mean transverse momentum of unpolarized quarks in a longitudinally polarized nucleon

$$\langle \vec{k}_\perp \rangle^q (\vec{b}_\perp) = \int \mathrm{d}x\, \mathrm{d}^2\vec{k}_\perp\, \vec{k}_\perp\, \rho^{[\gamma^+]q}(\vec{b}_\perp, \vec{k}_\perp, x, +\hat{e}_z). \tag{6}$$

The corresponding distributions for u and d quarks obtained within the LFCQM [4] are shown in Fig. 2. We clearly see that in a longitudinally polarized nucleon, the quarks have on average nonzero OAM. The u quarks tend to orbit anti-clockwise inside the nucleon, corresponding to $\ell_z^u > 0$ since the proton is represented with its spin pointing out of the figure. For the d quarks, we see two regions. In the central region of the nucleon, $b_\perp < 0.3$ fm, the d quarks tend to orbit anti-clockwise like the u quarks. In the peripheral region, $b_\perp > 0.3$ fm, the d quarks tend to orbit clockwise. The mean transverse momentum $\langle \vec{k}_\perp \rangle^q$ is always orthogonal to the impact-parameter vector $\vec{b}_\perp$. A non-zero radial component would indicate that the proton size and/or shape are changing. It can therefore only come from initial- and final-state interactions which affect the distribution of the struck quark before and after the hard interaction. Since such interactions are absent in our model, we do not see any radial contribution. If we consider the gauge-link contribution, we can obtain different definitions of the OAM from Eqs. (5)–(6),

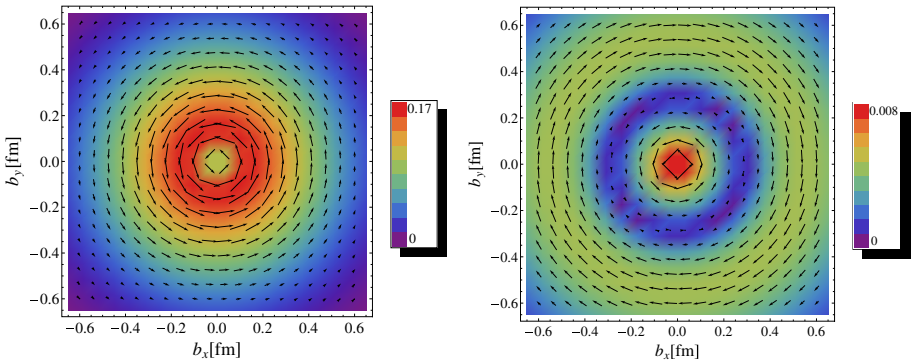

Figure 2. Distributions in impact-parameter space of the mean transverse momentum $\langle \vec{k}_\perp \rangle^q$ of unpolarized quarks in a longitudinally polarized nucleon. The nucleon polarization is pointing out of the plane, while the arrows show the size and direction of $\langle \vec{k}_\perp \rangle^q$. The left (right) panel shows the results for u (d) quarks.

depending on the shape of the Wilson line [9–12]. The gauge-invariant canonical OAM is obtained from Eqs. (3)–(4) using a staple-like gauge link connecting the points $-z/2$ and $+z/2$ via the intermediary points $-z/2 + \eta\infty^-$ and $z/2 + \eta\infty^-$ by straight lines, with the parameter η indicating whether the Wilson lines are future pointing ($\eta = +1$) or past pointing ($\eta = -1$) [5, 8]. In the light-front gauge $A^+ = 0$, Eq. (5) simply gives the Jaffe-Manohar OAM [13], *i.e.* $\frac{i}{2}\int \mathrm{d}^3\vec{r}\,\overline{\psi}^q\gamma^+(\vec{r}\times\overleftrightarrow{\partial}_{\vec{r}})_z\psi^q$. In contrast, if we connect the points $-z/2$ and $+z/2$ by a direct straight Wilson line, we obtain the kinetic OAM associated with the quark OAM operator appearing in the Ji decomposition [9, 14], *i.e.* $\frac{i}{2}\int \mathrm{d}^3\vec{r}\,\overline{\psi}^q\gamma^+(\vec{r}\times\overleftrightarrow{D}_{\vec{r}})_z\psi^q$, with $D_\mu = \partial_\mu - igA_\mu$ the usual covariant derivative.

References

[1] X. Ji, Phys. Rev. Lett. **91**, 062001 (2003)
[2] A.V. Belitsky, X. Ji and F. Yuan, Phys. Rev. D **69**, 074014 (2004)
[3] C. Lorcé and B. Pasquini B., Phys. Rev. D **84**, 014015 (2011)
[4] C. Lorcé, B. Pasquini, X. Xiong and F. Yuan, Phys. Rev. D **85**, 114006 (2012)
[5] S. Meissner, A. Metz and M. Schlegel, JHEP **0908**, 056 (2009)
[6] S. Meissner, A. Metz, M. Schlegel, and K. Goeke, JHEP **0808**, 038 (2008)
[7] C. Lorcé and B. Pasquini, JHEP **1309**, 138 (2013)
[8] C. Lorcé, B. Pasquini, and M. Vanderhaeghen, JHEP **1105**, 041 (2011)
[9] X. Ji, X. Xiong and F. Yuan, Phys. Rev. Lett. **109**, 152005 (2012)
[10] C. Lorcé, Phys. Lett. B **719**, 185 (2013)
[11] M. Burkardt, Phys. Rev. D **88**, 014014 (2013)
[12] E. Leader and C. Lorcé, `[arXiv:1309.4235 [hep-ph]]`
[13] R.L. Jaffe and A. Manohar, Nucl. Phys. B **337**, 509 (1990)
[14] X. Ji, Phys. Rev. Lett. **78**, 610 (1997)